Gap disturbances and regeneration patterns in a Bosnian old-growth forest: A multispectral remote sensing and ground-based approach.

Matteo Garbarino & Enrico Borgogno Mondino & Emanuele Lingua & Thomas A. Nagel & Vojislav Dukić & Zoran Govedar & Renzo Motta

Abstract

- ***Objectives***: We examined canopy gap structure and regeneration patterns at the landscape scale using a combination of remote sensing and field based surveys.
- ***Methods***: The study was carried out in the forest reserve of Lom, an old-growth *Fagus-Abies-Picea* forest located within the Dinaric Alps in the north-western part of Bosnia and Herzegovina. A high resolution (1-m Panchromatic and 4-m Multispectral) Kompsat-2 satellite image was orthorectified and classified through an unsupervised pixel based classification using an artificial neural network method.
- ***Results***: This approach allowed the identification of 650 canopy gaps, ranging in size from 32 to 1776 m^2. Only 20 intermediate to large gaps (> 250 m^2) were identified, and they were mainly present near the perimeter of the reserve. The origin of these large openings was associated with past human-caused disturbances or topographic conditions. The species composition of regeneration within large, human-caused gaps differed markedly from small gaps and non-gap sites in the core area of the reserve. Shade-intolerant species dominated the seedling and sapling layers in large openings. The landscape approach employed in this study confirmed the hypothesis that small gaps predominate at Lom, especially within the core area of the reserve.

Keywords

Canopy opening; gap-phase; primeval forest; spatial pattern; remote sensing; Balkan peninsula

1. Introduction

Forest disturbance and recovery strongly influence ecosystem processes and carbon balance both at regional and global scales. Disturbances influence successional pattern and process due to their extreme variability in size, frequency, and intensity (Turner et al. 1998). In temperate forests where large-scale, catastrophic disturbances are absent or very rare, dynamics are driven by the formation of small to intermediate scale openings in the forest canopy following mortality of canopy trees, often referred to as gap dynamics (Spies et al. 1990). Canopy gaps have a strong influence on forest dynamics because they increased light into the understory and drive tree recruitment to the canopy layer. They also contribute to the spatial heterogeneity of a forest landscape and are influenced by several climatic and physiographic factors that mainly act at the landscape level (Rich et al. 2010). However, little is known about canopy gap patterns and processes at the landscape scale, and only a few studies have addressed gap patterns at this scale (Battles et al. 1995; Hessburg et al. 1999; Smith and Urban 1988).

The spatial distribution of forest canopy gaps has important implications for understory light regimes and tree regeneration. Gap size and spatial distribution influence forest regeneration, and in turn, tree species diversity (Lawton and Putz 1988). Another important effect of the spatial distribution of canopy gaps is the creation of a mosaic of structural types within a forested landscape (Frelich and Lorimer 1991). Although spatial distribution is an important descriptor for forest disturbances such as canopy gaps, relatively few studies have investigated the spatial pattern of gap formation (e.g. Frelich and Lorimer 1991; Hessburg et al. 1999; Lawton and Putz 1988; Nuske et al. 2009).

A traditional approach to the study of gaps is based on field survey methods (for a complete review, see Schliemann and Bockheim 2011), which are limited in their ability to capture spatial and temporal patterns, and cannot be used extensively because of their financial cost (Vepakomma et al. 2008). An alternative approach is to employ remote sensing together with multiple scale ground surveys (Rich et al. 2010). Multispectral imagery can be a useful tool, but has rarely been used for canopy gap identification (Jackson et al. 2000). High resolution (e.g. < 5 m) spaceborne remote sensing data (e.g. Ikonos, QuickBird, Kompsat-2) provide a detailed view of forest canopies and are potentially useful tools to study canopy gaps at a variety of spatial scales

(Jackson et al. 2000; Rich et al. 2010). These aerial and satellite sensors permit automatic data collection enabling the sampling of broader areas and scales in the same period. Moreover, remote sensing analysis can be used to better structure the sampling design at a landscape scale.

In this study, we coupled high-spatial resolution Kompsat-2 satellite imagery from a single date with field observations in an old-growth mixed *Fagus-Abies-Picea* forest in Bosnia and Herzegovina. Such old-growth remnants in eastern and southeastern Europe provide valuable opportunities to evaluate small-scale tree mortality processes. Kompsat-2 digital imagery was chosen for the study because its geometric resolution approaches the scale of individual forest components, such as tree crowns and forest canopy gaps. Our specific objectives were: 1. to propose a classification method to detect complex gaps from satellite images and compare this approach with data collected in the field; 2. to quantify characteristics of canopy gaps, particularly gap spatial pattern, at the landscape scale; and 3. to understand the role of geometric attributes of gaps on forest regeneration.

2. Methods

2.1. Study area

The study was conducted in the Lom forest reserve. The reserve is a 297.8 ha area of old-growth forest (between 44°27' - 44°28' N, and 16°27' - 16°30' E, DATUM WGS84) located in the Dinaric Alps, within the Klecovača region in the north-western part of Bosnia and Herzegovina. The reserve has relatively gentle topography (1223-1503 m a.s.l.), but sinkholes are scattered throughout the area, which are typical features of the karst geology in the region. The climate is transitional continental with a mean annual temperature of 3.5°C and mean annual precipitation of 1600 mm, with maximum in December and minimum in July (Drinic climate station, 730 m a.s.l.). The forest reserve of Lom is divided in two zones, a core area of 55.8 ha that consists of well preserved old-growth (Motta et al. 2008; Motta et al. 2011) and a buffer zone that has some evidence of past human activities. Since 1956 all management activities are strictly forbidden in the entire reserve. The forest is dominated by silver fir (*Abies alba* Mill.), Norway spruce (*Picea abies* (L.) Karsten), and European beech (*Fagus sylvatica* L.), while sycamore maple (*Acer* *pseudoplatanus* L.) and Scots elm (*Ulmus glabra* Hudson) occur less frequently (Bucalo et al. 2007; Motta et al. 2008).

2.2. Image pre-processing and classification

A high resolution Kompsat-2 (Korea Multi-Purpose SATellite-2) satellite image was acquired on June 11, 2009. The acquired image is a Bundle type, comprising a 1-m GSD (Ground Sample Distance) panchromatic band (0.50-0.90 μm) and four 4-m GSD multispectral bands (Blue, Green, Red, Near Infrared). The sensor acquired the image with a 248.23° azimuth and an incidence angle of 6.44° and clouds were completely absent from the scene. The Kompsat-2 multispectral data were initially calibrated into reflectance at-the-ground values using the nominal values of Gain and Offset (Table 1) and applying the Dark Subtraction algorithm for a simplified atmospheric correction. These operations were performed using the ENVI software (ITT 2009). The satellite image was orthoprojected with the Toutin rigorous model for Kompsat-2 data implemented within the Orthoengine module of PCI software (PCIGeomatics 2009). 11 three dimensional Ground Control Points (GCPs), previously surveyed in the field with a Trimble GEOXM GPS, were used in this process. GPS pseudo-range code measurements were post-processed using the nearest permanent station (Sarajevo) belonging to the EUREF network. The resulting planimetric accuracy was about 1.5 m, sufficient enough for a 1:10,000 scale map. The digital elevation model used during the orthoprojection was the NASA/METI ASTER Global Terrain Model, with a geometric resolution of 30 m and vertical Root Mean Square Error (RMSE) of about 9 m. Both the panchromatic and the multispectral bands were orthoprojected obtaining a RMSE for the GCPs of 1.35 m.

The 1-m panchromatic band was used as an up to date map of the site to support surveys in the field. The 4-m multispectral image was used to test its suitability for canopy gap detection. A sub-sample of the area surrounding the forest reserve of 12612 ha was selected for this purpose. To obtain a high degree of automation we adopted an unsupervised pixel-based classification method in place of an object-oriented one. In optical remote sensing, especially when using a pixel-based classification approach, dark shadows cast by larger crowns adjacent to smaller trees or edge canopies into a canopy gap can be a significant problem and hence can make it difficult to reliably quantify gap characteristics (Asner et al. 2003; Leboeuf et al. 2007). Bands ratios such as NDVI (Normalized Difference Vegetation Index) can be used to limit the effect of shadows and illumination differences without losing the physical meaning of the investigated object (canopy). In fact the NDVI is considered relatively insensitive to changes in shadow fraction (Asner et al. 2003). Thus, an NDVI image was generated from the Red and NIR bands and stacked together with the four original bands. Five bands were then used during the classification.

The proposed approach tests the ability of an unsupervised pixel-based classification to separate the class 'canopy gap' from the remaining vegetation. The classifier used for this task is based on the Artificial Neural Networks (ANN) philosophy. In particular, we used the Neural Gas algorithm which was specifically developed with IDL (Interactive Data Language) routine. The unsupervised classifier was applied twice successively. First, the image was classified into 16 classes that were subsequently aggregated into 7 classes following the Jeffries-Matusita separability test. Second, two textural occurrence measures (i.e. data range and standard deviation) were generated with a 7x7 kernel for each of the original bands. The new 10 band image was first masked to address the operation to the 'gap' class pixels, then clustered through the NG algorithm into 2 clusters. This permitted the separation of the large and homogeneous openings (meadows in our case) from forest canopy gaps. A polygon vector canopy gap map (Fig. 1) was derived from the final classification image in a GIS environment adopting a minimum mapping unit (MMU) of two pixels (32 m^2). The class 'canopy gap' comprised those openings in the forest canopy dominated by soil, grasses, and coarse woody debris where the gap-filling process by tree regeneration was in its early phase. From an image processing point of view a "gap" can be considered as a local spectral and textural anomaly within the forest class. The accuracy of the canopy gap map was assessed through two different approaches: field observations of 40 sample gaps were used to evaluate the underestimation of canopy gaps and a visual check of all classified gaps (n = 360) on a false color RGB composite was done to assess the potential overestimation of gaps. One hundred percent of the visited gaps were correctly classified. The visual check revealed that 82 % of gaps were correctly classified, and 8 % were uncertainly classified. Moreover, the spectral signature of the whole 'canopy gap' class was compared to the spectral characteristics of 18 photointerpreted gaps in order to test the ability of the classification to detect real canopy gaps. The spectral statistics for the class ‘canopy gap’ were very similar to the spectral statistics of the photointerpreted gaps (Fig. 2).

2.3. Spatial pattern of canopy gaps

Because canopy gaps are objects with finite size and irregular shape and they can be large in comparison to the investigated spatial scales we treated the gaps as patches or polygons avoiding point approximation (Wiegand et al. 2006). Three different categorical raster maps (i.e. the whole reserve, buffer zone, and core area) of 4-m spatial resolution were derived from the canopy gap vector map obtained from the satellite image. The categorical maps were transformed to a matrix with 2 categories (canopy gaps, and forest) and a mask was used to take into account the irregular shape of the study area (space restriction effect). In order to analyse the spatial pattern of gaps we used both Ripley’s *L*-function (Ripley 1976) and the *O*-ring statistic (Wiegand et al. 1999). This latter was computed as complementary analysis to avoid the misinterpretation of results due to the cumulative effect of Ripley’s index that can confound effects at larger distances with effects at shorter distances (Perry et al. 2006). Complete spatial randomness (CSR) was chosen as a null model built by rotating and moving the objects within the raster map. All the spatial analyses were performed using the Programita software (Wiegand and Moloney 2004).

2.4. Gap geometry and forest regeneration

The influence of gap geometry (size, shape, and direction) on regeneration structure and composition was assessed through field surveys. The orthorectified Kompsat-2 image was used to locate larger gaps (> 200 m2) in order to include additional samples to an existing dataset (Bottero et al. 2011) of 56 canopy gaps (ranging from 11 to 708 m2). Data on regeneration structure and composition were collected and georeferenced with a GPS. The density of seedlings (trees < 1 m height), saplings (trees > 1 m tall and with diameter at the breast height < 7.5 cm), and gap fillers (trees > 7.5 dbh and less than 20 m tall) was measured within a 6 m radius circular plot located in the centroid of each canopy gap. Gap size was calculated in a GIS environment using the triangles method based on the mapped position on the ground of the trees bordering the gap. The shape was measured as direction expressed as north-eastness index and elongation of polygons by using the Longest Straight Line extension for ArcView 3.x (Jenness 2007).

The relationship between regeneration composition and gap geometry was analyzed through redundancy analysis (RDA) (Rao 1964). This direct gradient analysis is a constrained ordination method that was used to investigate the variability explained by the explanatory variables and their correlation with regeneration composition variation. Two data sets were used in this ordination analysis: (a) regeneration composition (10 species x 60 plots); and (b) geometry of canopy gaps (5 variables x 60 plots). The RDA was performed using Canoco® (ter Braak and Smilauer 1998), and the statistical significance of all ordination analyses was tested by the Monte Carlo permutation method based on 10000 runs with randomized data.

3. Results

3.1. Canopy gaps characteristics

A total of 650 canopy gaps were located by multispectral remote detection within the Lom forest reserve (Table 2). The average size of these gaps was 78.2 m^2 and the variability observed was high, ranging from 32 to 1776 m^2. The total gap area was 5.1 ha, resulting in a gap fraction of 1.7 % and the density of canopy gaps within the whole reserve was 2.2 ha^{-1}.

The core area and buffer zone differed in canopy gap density (1.7 and 2.3 ha^{-1} respectively) and mean size (62.6 and 81.2 ha^{-1} respectively). The average gap area was strongly influenced by the different size of the largest gap in the two zones (320 m^2 in the core area and 1776 m^2 in the buffer zone). Moreover, the variability of gap area was much smaller (50 m^2 standard deviation) in the core area than in the buffer zone (106.7 m^2 standard deviation).

The frequency distribution of canopy gap size in both the core area and buffer zone (Fig. 3) followed a negative exponential form with smaller gaps more frequent than larger ones. The difference in size distribution between the two zones was not significant (Komolgorov-Smirnov test, p = 0.116). The proportion of gaps smaller than 100 m^2 differed slightly between the core area (89%) and the buffer zone (80%), and the amount of gaps larger than 300 m^2 was similar in the two zones (4% core area; 6.6% buffer zone).

3.2. Spatial pattern of canopy gaps

The spatial distribution of canopy gaps varied in the different parts of the Lom reserve. The univariate Ripley's L-function for the whole reserve showed a deviation from complete spatial randomness starting at a distance of 20 m (Fig. 4e). Spatial patterns between the buffer zone and the core area were different. In the core area the L-function values stay within the confidence envelope (Fig. 4a), indicating a random distribution of the canopy gaps at all scales (0 to 200 m). In the buffer zone the spatial pattern of the gaps was clustered for distances larger than 20 m (Fig. 4c). The results are consistent with the O-ring analysis (Fig. 4b, d, f).

3.3. Gap geometry and forest regeneration

Silver fir was the dominant species in the seedling layer, beech in the sapling one, and Norway spruce, rowan and maple were denser in large and elongated gaps (Table 3). The redundancy analysis revealed that gap geometry was related to regeneration composition (Fig. 5). The first and second axes accounted for 10.4 and 1.6 % of the total variation, respectively (Table 4). Early-successional and shade-intolerant species, such as sycamore maple and rowan, were positively associated with large (Area, Perimeter) and elongated (Long) gaps. European beech saplings were not influenced by gap size, but were weakly associated to gap filler basal area. The different pattern observed for rowan seedlings (Sorbus_1) and saplings (Sorbus_2) was probably due to the fact that this species is shade-tolerant only in the first stages of its life.

4. Discussion and conclusion

4.1. Gap delineation using high resolution multispectral data

In this study, high-spatial resolution Kompsat-2 satellite imagery was coupled with field data to assess important components of the gap disturbance regime across a temperate mixed forest landscape. Our results indicate that it is possible to measure key components of gaps using spectral and textural features from high-spatial resolution data. The 650 identified gaps were dominated by grasses, forbs, bare soil and coarse woody debris, indicating that the classification method adopted in this study picked out predominately recently formed gaps. This explains the very low gap fraction observed in the study compared to those values (often > 10%) reported in studies of similar forests in Europe (Drösser and von Lüpke 2005; Nagel and Svoboda 2008; Splechtna et al. 2005) and in a companion study (Bottero et al. 2011). Typically, field based surveys of gaps distinguish openings from closed canopy areas by using a height cutoff of gapfilling trees, often around half the height of the main canopy layer. The minimum gap size considered in the present study (32 m^2) was larger than the threshold adopted in many field based surveys. Consequently, these studies sample a broad range of gap ages and sizes, resulting in a higher gap fraction.

The NDVI was calculated to help in the classification process, but there was a low correlation between the index and the disturbed surfaces. The weak relationship observed was mainly due to the fact that vegetation (e.g. forest regeneration, shrubs, and grasses) was present beneath the forest canopy and within the openings. Forest canopy gaps with dense understory vegetation likely have a similar near infrared response to a closed canopy site, particularly for gaps in the later stages of the gapfilling process with gap fillers reaching the lower canopy layer. Nevertheless, disturbed sites like canopy gaps often have rougher texture and are more heterogeneous than closed canopy areas (Rich et al. 2010). To overcome the limits of spectral data, textural features were subsequently used to improve the automatic classification method. Although the classification method proved to be useful, a substantial improvement for canopy gap detection can be obtained through the use of LiDAR imagery (Gaulton and Malthus 2010; Vepakomma et al. 2008). However, the automatic classification on high resolution multispectral data presented in this study proved to be a good estimator of recently formed canopy gaps and it is more cost effective than LiDAR. Another advantage of multispectral satellite imagery is the possibility of performing a diachronic study on a series of historical satellite images.

4.2. Spatial pattern of canopy gaps

The spatial pattern observed in our study site seems follow these findings. The gaps within the core area of the Lom reserve were randomly distributed, which is likely due to the relative environmental homogeneity of the area and the lack of recent higher severity disturbance events. Consistently, a large proportion of the gaps in the core area were formed by endogenous mortality of large canopy trees (Bottero et al. 2011). The random spatial distribution of canopy gaps found in Lom's core area is in agreement with other studies in temperate forests (Frelich and Lorimer

1991; Nuske et al. 2009). In contrast, gaps were larger and clustered in the surrounding buffer zone, which is due to topographic and human caused influences. A higher density of gaps was found at higher elevations in close proximity to the ridges of the reserve. This may be partly because these areas are more wind exposed, but also due to several artificial gaps from recent (1992-1995 Bosnian War) illegal logging and former grazing activities. These artificial openings were located in close proximity to manmade trails and dirt roads, which likely contributed to the clumped pattern of gaps.

4.3. Forest regeneration as influenced by canopy gap geometry

First, it should be noted that the gap size range observed in Lom (32-1700 m2) was similar to the size distribution of gaps commonly reported for forests where small-scale disturbance events occur (Lawton and Putz 1988; Lertzman and Krebs 1991; Nagel and Svoboda 2008; Spies et al. 1990). Gap size had little influence on regeneration density in Lom, which was also found in a companion study (Bottero et al. 2011). This finding is confirmed by other studies in southeastern European forests, where the presence of a stratum of advance regeneration partially explains the weak relationship between regeneration density and gap size. Other factors such as gap age seem to be related to seedling density more than gap size, probably due to thinning and architectural differences between species over time due to competition (Poulson and Platt 1989; Spies et al. 1990).

The results from our study area partially confirmed a conceptual gap model that predicts an increase in the relative dominance of shade-intolerant species as size of disturbance increases (Runkle 1985). Gap geometry (size, direction, and shape) had very little influence on the occurrence of shade-tolerant species such as *P. abies*, *F. sylvatica*, and *A. alba*, because they were already present as advance regeneration before gap formation. Thus, it was not surprising to observe that forest canopy gaps were not primary sites of regeneration, but mainly acted in regulating the recruitment of advance regeneration dominated by shade-tolerant species (Busing and White 1997). Less shade-tolerant species, such as *A. pseudoplatanus* and *S. aucuparia* were present only in lager gaps and were dominant in only a few artificial openings located in the buffer zone of the reserve. Large canopy gaps are important for the maintenance of shade-intolerant species that are more competitive in open areas (Whitmore 1989) and occur only in small numbers in closed canopy forests.

Acknowledgements and funding

Spot Image Inc., through Planet Action Program domain 'Forest and deforestation', provided funding for this research by donating satellite imagery and image processing systems.

The assistance with field surveys of Miroslav Svoboda of the Czech University of Life Sciences Prague, Tihomir Rugani, and Dejan Firm of the University of Ljubljana, and Fabio Meloni, Roberta Berretti, Daniele Castagneri, and Alessandra Bottero of the University of Torino, is appreciated.

References

Asner GP, Warner AS (2003) Canopy shadow in IKONOS satellite observations of tropical forests and savannas. Remote Sens Environ 87:521-533

Battles JJ, Fahey TJ, Harney EMB (1995) Spatial patterning in the canopy gap regime of a subalpine Abies-Picea forest in the northeastern United States. J Veg Sci 6:807-814

Bottero A, Garbarino M, Dukic V, Govedar Z, Lingua E, Nagel TA, Motta R (2011) Gap-phase dynamics in the old growth forest of Lom (Bosnia-Herzegovina). Silva Fennica 45(5)

Bucalo V, Brujic J, Travar J, Milanovic D (2007) Survey of flora in the virgin reserve "Lom". Bulletin of Faculty of Forestry University of Belgrade 95:35-48

Busing RT, White PS (1997) Species diversity and small-scale disturbance in an old-growth temperate forest: a consideration of gap partitioning concepts. Oikos 78:562–568

Drösser L, von Lüpke B (2005) Canopy gaps in two virgin beech forest reserves in Slovakia. J Forest Sci 51:446–457

Frelich L, Lorimer CG (1991) Natural disturbance regimes in Hemlock-Hardwood forests of the Upper Great Lakes region. Ecol Monogr 61:145-164

Gaulton R, Malthus TJ (2010) LiDAR mapping of canopy gaps in continuous cover forests: A comparison of canopy height model and point cloud based techniques. Int J Remote Sens 31:1193-1211

Hessburg PF, Smith BG, Salter RB (1999) Detecting change in forest spatial patterns from reference conditions. Ecol Appl 9:1232-1252

ITT (2009) ENVI 4.7. ITT Visual Information Solutions, Boulder, CO

Jackson RG, Foody GM, Quine CP (2000) Characterising windthrown gaps from fine spatial resolution remotely sensed data. For Ecol Manag 135:253-260

Jenness J (2007) Longest straight lines across the interior of polygons. Jenness Enterprises, Flagstaff, AZ

Lawton OR, Putz FE (1988) Natural disturbance and gap-phase regeneration in a wind-exposed tropical cloud forest. Ecology 69:764-777

Leboeuf A, Beaudoin A, Fournier RA, Guindon L, Luther JE, Lambert M-C (2007) A shadow fraction method for mapping biomass of northern boreal black spruce forests using QuickBird imagery. Remote Sens Environ 110:488-500

Lertzman KP Krebs CJ (1991) Gap-phase structure of subalpine old-growth forest. Can J For Res 21:1730-1741

Motta R, Maunaga Z, Berretti R, Castagneri D, Lingua E, Meloni F (2008) La riserva forestale di Lom (Repubblica di Bosnia Erzegovina): descrizione caratteristiche struttura di un popolamento vetusto e confronto con popolamenti stramaturi delle Alpi italiane. Forest@ 5:100-111

Motta R, Berretti R, Dukić V, Garbarino M, Govedar Z, Lingua E, Maunaga Z, Meloni F (2011) Toward a definition of the range of variability of central European mixed Fagus–Abies–Picea forests: the nearly steady-state forest of Lom (Bosnia and Herzegovina). Can J For Res 41: 1871–1884

Nagel TA, Svoboda M (2008) Gap disturbance regime in an old-growth Fagus–Abies forest in the Dinaric Mountains Bosnia-Herzegovina. Can J For Res 38:2728–2737

Nuske RS, Sprauer S, Saborowski J (2009) Adapting the pair-correlation function for analysing the spatial distribution of canopy gaps. For Ecol Manag 259:107-116

PCI Geomatics (2009) Geomatica 10.3, Richmond Hill, ON

Perry GLW, Miller BP, Enright NJ (2006) A comparison of methods for the statistical analysis of spatial point patterns in plant ecology. Plant Ecol 187:59-82

Poulson TL, Platt WJ (1989) Gap light regimes influence canopy tree diversity. Ecology 70:553-555

Rao CR (1964) The use and interpretation of principal components analysis in applied research. Sankhya 26:329-358

Rich RL, Frelich L, Reich PB, Bauer ME (2010) Detecting wind disturbance severity and canopy heterogeneity in boreal forest by coupling high-spatial resolution satellite imagery and field data. Remote Sens Environ 114:299-308

Ripley BD (1976) The Second-Order Analysis of Stationary Point Processes. J Appl Probab 13:255-266

Runkle JR (1985) Disturbance regimes in temperate forests. Academic Press, Orlando

Schliemann SA, Bockheim JG (2011) Methods for studying treefall gaps: A review. For Ecol Manag 261:1143-1151

Smith TM, Urban DL (1988) Scale and resolution of forest structural pattern. Vegetatio 74:143-150

Spies TA, Franklin JF, Klopsch M (1990) Canopy gaps in Douglas-fir forest of the Cascade mountains. Can J For Res 20:649-658

Splechtna BE, Gratzer G, Black BA (2005) Disturbance history of a European old-growth mixed-species forest—A spatial dendro-ecological analysis. J Veg Sci 16:511-522

ter Braak, CJF, Smilauer P (1998) Reference Manual and User's Guide to Canoco for Windows: Software for Canonical Community Ordination (version 4), Ithaca, NY

Turner MG, Baker WL, Peterson CJ, Peet RK (1998) Factors influencing succession: lessons from large infrequent natural disturbances. Ecosystems 1:511-523

Vepakomma U, St-Onge B, Kneeshaw D (2008) Spatially explicit characterization of boreal forest gap dynamics using multi-temporal lidar data. Remote Sens Environ 112:2326-2340

Whitmore TC (1989) Canopy gaps and the two major groups of forest trees. Ecology 70:536-538

Wiegand T, Moloney KA, Naves J, Knauer F (1999) Finding the missing link between landscape structure and population dynamics: a spatially explicit perspective. Am. Nat. 154: 605-627

Wiegand T, Moloney AK (2004) Rings, circles, and null-models for point pattern analysis in ecology. Oikos 104: 209-229.

Wiegand T, Kissling WD, Cipriotti PA, Aguiar MR (2006) Extending point pattern analysis for objects of finite size and irregular shape. J Ecol 94:825-837

Tables

Table 1. Nominal coefficients used for the calibration to surface reflectance of the Kompsat 2 image.

Band	L max ($W/(m^2.sr.\mu m)$)	L min ($W/(m^2.sr.\mu m)$)	Sun Irradiance ($W/(m^2.sr.\mu m)$)	Central wavelength (μm)
1 (Blue)	-1.52	193.00	1929.00	0.485
2 (Green)	-2.84	365.00	1837.00	0.560
3 (Red)	-1.17	264.00	1556.00	0.660
4 (NIR)	-1.51	221.00	1068.00	0.830

Table 2. Landscape metrics and statistics of geometrical attributes of canopy gaps of the Lom old-growth forest in Bosnia Herzegovina.

Metrics	Unit	Core area	Buffer Zone	Reserve
Total area	ha	55.8	242.0	297.8
Number of gaps	n	102	548	650
Density of gaps	n/ha	1.7	2.3	2.2
Minimum gap area	m^2	32.0	32.0	32.0
Maximum gap area	m^2	320.0	1776.0	1776.0
Mean gap area	m^2	62.6	81.2	78.2
Median gap area	m^2	48.0	48.0	48.0
Stdv. gap area	m^2	50.0	106.7	100.2
Minimun gap perimeter	m	24.0	24.0	24.0
Maximum gap perimeter	m	96.0	368.0	368.0
Mean gap perimeter	m	35.1	40.8	39.9
Stdv. gap perimeter	m	15.1	27.6	26.1
Gap fraction	%	1.08	1.85	1.70

Table 3. Gap geometry characteristics and seedlings (1) and saplings (2) species composition (*Abies* = silver fir; *Fagus* = European beech; *Picea* = Norway spruce; *Acer* = sycamore maple; *Sorbus* = rowan) divided by 4 classes of canopy gaps' area.

Gap area classes (m^2)	< 50	50-100	100-250	>250	Total
Number of gaps	21	14	16	7	58
Gap area mean (m^2)	25.64	74.66	145.47	670.80	139.22
Gap area standard deviation (m^2)	13.75	14.69	36.42	142.11	196.07
Gap perimeter (m)	20.79	37.29	54.01	147.75	47.53
Gap elongation (m)	8.23	14.06	19.41	38.92	16.03
Gap fillers (m^2/ha)	7.28	7.88	9.75	9.08	8.31
Regeneration composition (n/ha)					
Picea_1	640	783	619	1120	719.77
Picea_2	17	227	133	1238	229.58
Abies_1	4143	4446	3890	3183	4045.58
Abies_2	152	303	133	2476	428.14
Fagus_1	1196	1036	1326	1415	1216.15
Fagus_2	825	884	884	1592	936.94
Acer_1	337	51	354	589	297.83
Acer_2	0	25	0	0	6.20
Sorbus_1	118	0	155	589	148.92
Sorbus_2	0	0	0	236	24.82

Table 4. Correlation of gap geometry variables with the first four axes of the regeneration composition RDAs. Boldface numbers represent the correlations greater than 0.3 between explanatory variables and the ordination axes. A *p* value of 0.004 on the significance of all canonical axes is derived from a Monte Carlo test with 10000 permutations.

Axis	RDA-1	RDA-2	RDA-3	RDA-4
% of variance	10.4	1.6	1.2	0.3
Species-environment correlations	0.74	0.39	0.31	0.16
Area (gap area)	**0.59**	0.17	0.09	-0.04
Perimeter (gap perimeter)	**0.52**	0.14	0.15	-0.03
Long (gap elongation)	**0.59**	0.06	0.07	-0.01
NE (gap direction)	0.16	0.03	0.12	0.13
Fillers (gap fillers basal area)	-0.20	**0.30**	-0.08	0.01

Figure captions

Fig. 1 Canopy gap map of the Lom forest reserve showing the geographic distribution of canopy gaps (minimum mapping unit = 32 m^2) bounded by the core area and the forest reserve borders. Example Kompsat-2 subset images reporting the zoom of a single canopy gap as observed on (A) the panchromatic (1-m resolution) and (B) the multispectral image are also showed.

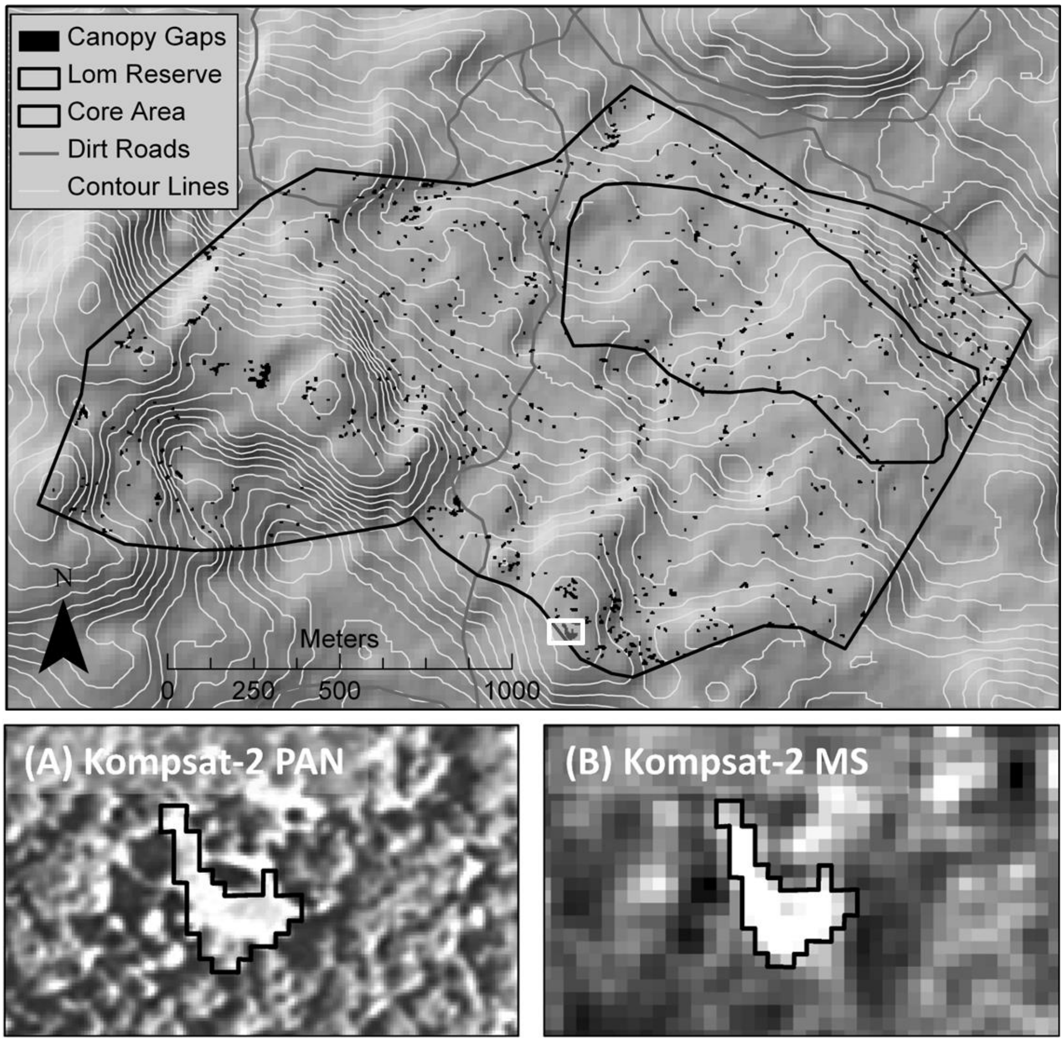

Fig. 2 Comparison between spectral mean values of classified gaps (class ‘canopy gap’) and 18 photointerpreted gaps from the Kompsat-2 image. Error bars represent standard deviation of spectral features.

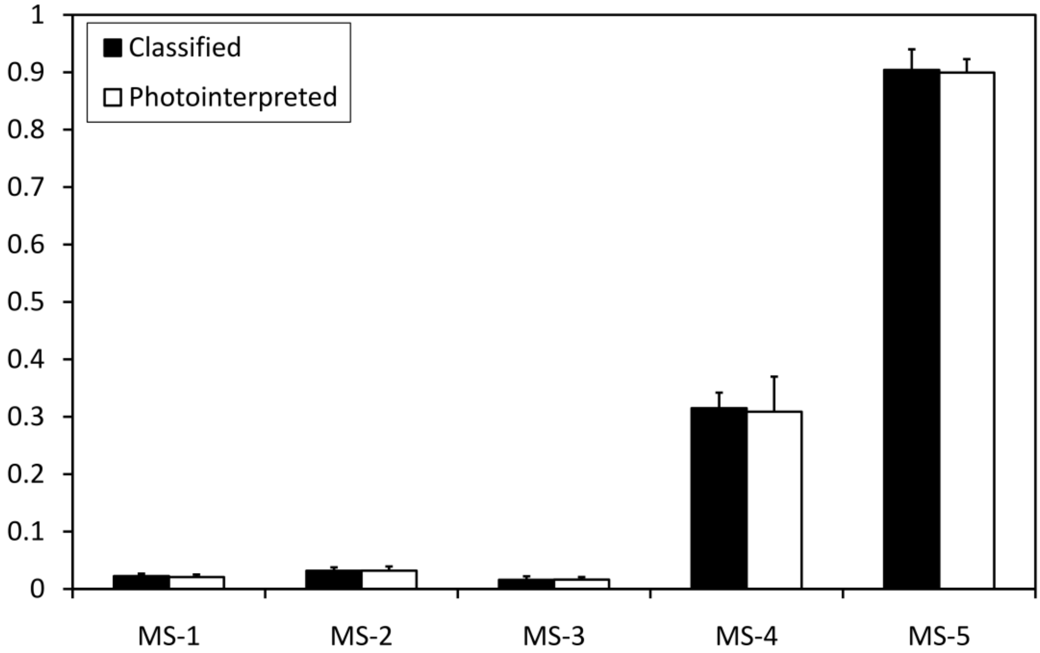

Fig. 3 Frequency distribution of canopy gap size in the core area and in the buffer zone of the Lom forest reserve in Bosnia and Herzegovina.

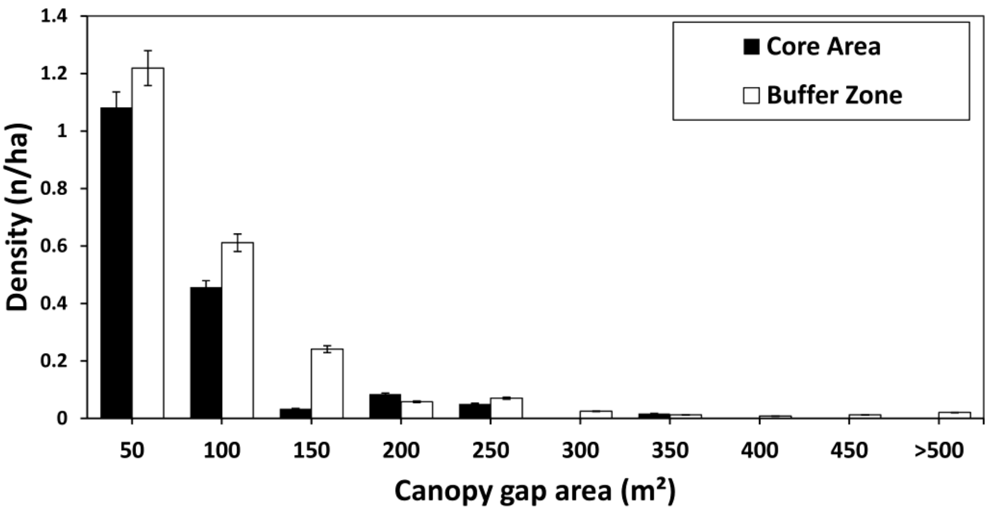

Fig. 4 Univariate Ripley's L-functions -*L(d)*- and O-ring pair-correlation functions -*O(r)*- of the canopy gaps of the Lom old-growth forest using the polygon-based approach respectively in the core area (a, b), the buffer zone (c, d), and the whole reserve (e, f). Black line: estimated function; dotted lines: upper and lower confidence envelopes under the null hypothesis of complete spatial randomness, computed by Monte Carlo simulation using 1000 replicates.

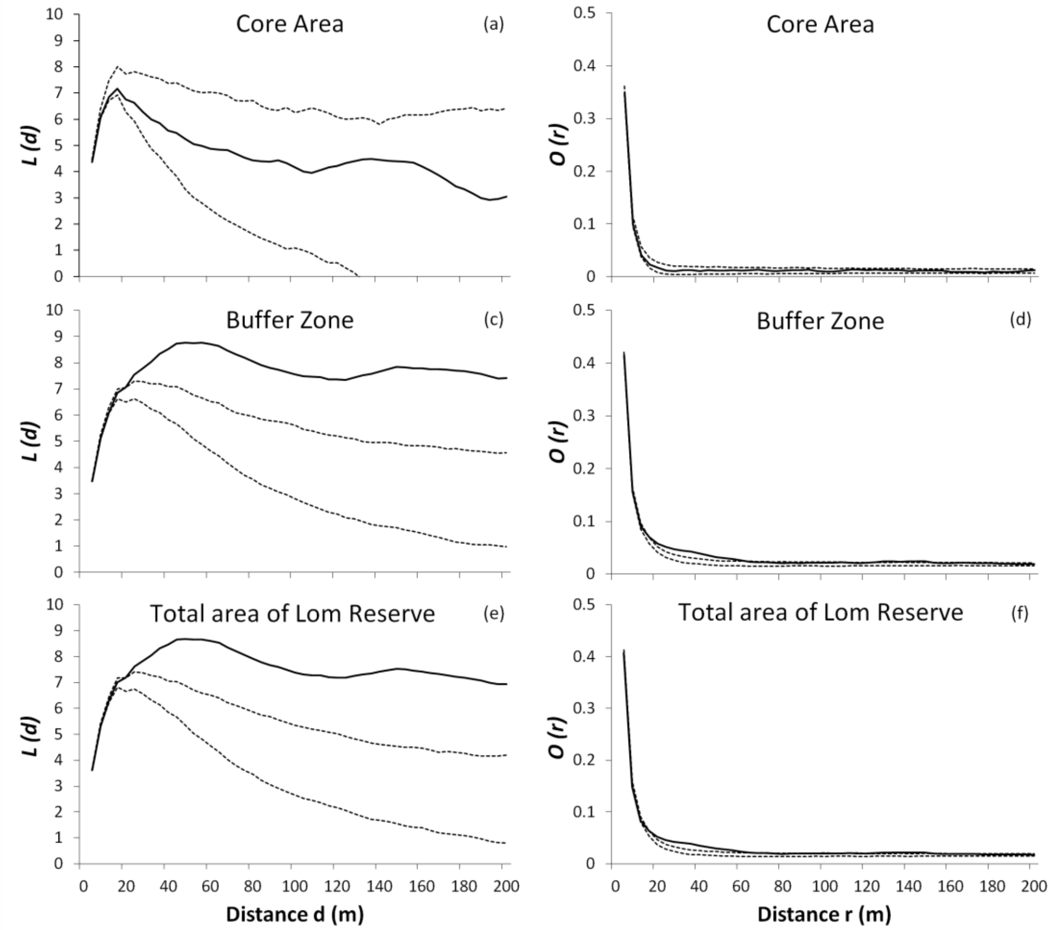

Fig. 5 Redundancy analysis (RDA of 60 plots) of regeneration composition in relation to canopy gap geometry and gap filler basal area. Dashed arrows show the tree species (*Abies* = silver fir; *Fagus* = European beech; *Picea* = Norway spruce; *Acer* = Sycamore maple; *Sorbus* = Rowan) divided by seedlings (1) and saplings (2). Solid line arrows represent the "biplot scores of canopy gaps geometry" (Perimeter = gap perimeter; Area = gap area; Long = longest straight line across the interior of a gap; NE = north-eastness index of gap direction) and gap filler basal area (Fillers). A p value of 0.004 on the significance of all canonical axes is derived from a Monte Carlo test with 10000 permutations.